

Drift Region Voltage Drop in SiC VDIMOS - The Influence of Anisotropy

Abedalhakem Alkowash
University of Sabratha, Faculty of Engineering, Sabratha

Abstract

Silicon Carbide (SiC) is an important indirect wide band gap semiconductor with outstanding electronic properties. This work focuses on an investigations of silicon carbide (SiC) based vertical Double Implanted Metal Oxide Semiconductor Field Effect Transistor (DIMOSFET). Silicon Carbide (4H SiC as well as 6H SiC) is known to be highly anisotropic material. Among others, the transport parameters like low field mobility and saturation velocity are considerably different in c direction compared to a and b directions. The aim of this paper is to investigate the influence of variation of mentioned parameters, as well as the variation of parameters describing specific model, on "drift region voltage drop" in vertical DIMOS structure.

Keywords: DIMOSFET, SiC, Transport parameters, SiC anisotropy, drift region voltage drop.

1. Introduction

In the last fifteen years, silicon-carbide (SiC) has emerged as one of the most promising semiconductor materials for design and fabrication of different devices widely used in microelectronics and nanoelectronics [1]. It turned out to be extremely successful in overcoming the limitations and shortcomings of Si-based devices. Due to its superior thermal and electric properties and satisfactory transport performances if compared to silicon, silicon-carbide has become a promising candidate for use in high-temperature and high-power, as well as in switching devices. One of the best developed structures is a vertical double implanted metal oxide semiconductor (field effect) transistor. It can carry large currents during "on" state, while its vertical section (drift region) is capable of sustaining large blocking voltages in the "off" state [2]. In spite of many papers reporting on the investigation of such structures, their level of development can still be regarded as modest and insufficient. Therefore, the aim of this paper is to include the anisotropic character and temperature dependence of transport parameters such as low field mobility and saturation velocity, as well as the behavior of parameter β describing specific features of drift-diffusion transport model in silicon and similar materials [3]-[13]. The focus of the paper is on vertical section (drift region), and its investigation has been carried out analytically as long as possible. The horizontal channel itself has been described and modeled in many conventional MOS-structures, hence no special attention has been paid to it in this paper.

2. Theoretical Basis of "Drift" Region Model

The conventional vertical SiC DIMOSFET investigated in this paper is shown in figure 1. The domain of interest is a vertical "drift" region and it is assumed to be divided into three sections A, B, C (figure 1.). The total current in each of these three regions should be the same. It is vertical and equal to drain current. The previous analyses of "drift" region have led to the development of its widely accepted model

suggesting following expressions for voltage drop in each of its sections [2]:

$$V_B = \frac{I_D \cdot W_A}{e \cdot W \cdot N_D \cdot \mu_n \cdot L_d - \frac{I_D}{E_C}} \quad (1a)$$

$$V_B = \frac{I_D}{2 \cdot W \cdot e \cdot N_D \cdot \mu_n \cdot ct \, g \, \alpha} \cdot \ln \frac{e \cdot W \cdot N_D \cdot \mu_n \cdot (L_d + L_P) - \frac{I_D}{E_C}}{e \cdot W \cdot N_D \cdot \mu_n \cdot L_d - \frac{I_D}{E_C}} \quad (1b)$$

$$V_C = \frac{I_D \cdot \left(W_T - W_j - W_d - \frac{L_P}{2} \cdot t \alpha \right)}{W \cdot e \cdot N_D \cdot \mu_n \cdot (L_d + L_P) - \frac{I_D}{E_C}} \quad (1c)$$

where W_A is the accumulation region depth, W_T is the total thickness of epilayer, L_d is the accumulation region length, L_P is the p-body length, N_D is the concentration of the ionized donors, $W_A = W_j + W_d$, μ_n is the low field mobility, $E_c = v_s/\mu_n$ Other geometric parameters are labeled in figure 1.

Describing carriers' transport in silicon unipolar devices. This model is realized from equation (2) with the limited number of parameters to be fitted to the experimental data. It also provides the analytical treatment of its expressions far enough, as well as its straightforward implementation in more complex circuit simulation. But this model also suffers from serious shortcomings to be dealt with in this paper. First, silicon-carbide (both 4H-SiC and 6H-SiC) is known to be a highly anisotropic material, i. e. its transport properties, and hence corresponding coefficients, are different in \underline{c} -direction compared to \underline{a} and \underline{b} directions. These coefficients also depend on the operating temperature, what begins to play an important role having on mind that silicon-carbide devices are supposed to be used in the high temperature range. The model can also be improved by introducing the parameter β responsible for transport characteristic $v(E)$ fine tuning. The parameter itself is also anisotropic and shows the considerable temperature dependence [3], [4].

The modern literature concerning drift-diffusion model suggests replacing the expression (2) by a more detailed one [3]:

$$v = \frac{\mu_n \cdot E_x}{\left[1 + \left(\frac{\mu_n}{v_s} \cdot E_x\right)^\beta\right]^{1/\beta}} = \frac{\mu_n \cdot \frac{dV}{dx}}{\left[1 + \left(\frac{\mu_n}{v_s} \cdot \frac{dV}{dx}\right)^\beta\right]^{1/\beta}} \quad (3)$$

This formula is also consistent with the main features of hydrodynamic model, which is based on the Boltzmann transport equation and its moments leading to balance equations. Therefore, the relation (3) can be regarded as a product of serious theoretical consideration rather than the consequence of simple fitting to the experimental data. Once having this formula adopted, its implementation in the "drift region" model causes no unavoidable difficulties in its accumulation layer A:

$$I_D = e \cdot W \cdot N_D \cdot L_d \cdot v$$

$$= \frac{e \cdot N_D \cdot \mu_n \cdot W \cdot L_d \cdot \frac{dV}{dx}}{\left[1 + \left(\frac{\mu_n}{v_s} \cdot \frac{dV}{dx}\right)^\beta\right]^{1/\beta}} \quad (4a)$$

Straight-forward leading to expressions:

$$\frac{dV}{dx} = \frac{I_D}{\left[(e \cdot W \cdot N_D \cdot L_d \cdot \mu_n)^\beta - \left(\frac{\mu_n \cdot I_D}{v_s}\right)^\beta\right]^{1/\beta}} \quad (4b)$$

and:

$$V_A = \frac{I_D \cdot W_A}{\left[(e \cdot W \cdot N_D \cdot L_d \cdot \mu_n)^\beta - \left(\frac{\mu_n \cdot I_D}{v_s} \right)^\beta \right]^{1/\beta}} \quad c)$$

The calculation of the voltage drop over varying cross-section layer B causes some more effort:

$$I_D = \frac{e \cdot N_D \cdot \mu_n \cdot W \cdot [L_d + (x - V_A) \cdot ctg\alpha] \cdot \frac{dV}{dx}}{\left[1 + \left(\frac{\mu_n}{v_s} \cdot \frac{dV}{dx} \right)^\beta \right]^{1/\beta}} \quad (5a)$$

and hence:

$$- \int_{W_A}^{W_A + \frac{L_p}{2} \cdot ctg\alpha} \frac{I_D \cdot dx}{\left\{ [e \cdot W \cdot N_D \cdot \mu_n \cdot (I_D + 2 \cdot (x - W_A) \cdot ctg\alpha)]^\beta - \left(\frac{\mu_n \cdot I_D}{v_s} \right)^\beta \right\}^{1/\beta}} \quad V_B \quad (5b)$$

The above expression becomes simpler after introducing a new variable:

$$e \cdot W \cdot N_D \cdot \mu_n \cdot [L_d + 2 \cdot (x - W_A) \cdot ctg\alpha] = z \quad (5c)$$

whit a result:

$$V_B = \frac{I_D \cdot \operatorname{tg} \alpha}{2 \cdot e \cdot W \cdot N_D \cdot \mu_n} \int_{e \cdot W \cdot N_D \cdot \mu_n \cdot L_d}^{e \cdot W \cdot N_D \cdot \mu_n (L_d + L_p)} \frac{dz}{\left[z^\beta - \left(\frac{\mu_n \cdot I_D}{v_s} \right)^\beta \right]^{1/\beta}} \quad (5d)$$

The analytical evaluation of V_B would be possible if we used approximate values for coefficient β . But, the procedure is tedious and hence not worth performing. It is much more convenient to calculate V_B by means of any of adequate software tools (MATHLAB, MATHEMATICA...). The expression for V_B can be reorganized as follows:

$$V_B = \frac{I_D \cdot \operatorname{tg} \alpha}{2 \cdot e \cdot W \cdot N_D \cdot \mu_n} \cdot \{f[e \cdot W \cdot N_D \cdot \mu_n (L_d + L_p)] - f(e \cdot W \cdot N_D \cdot \mu_n \cdot L_d)\} \quad (6a)$$

With the abbreviation:

$$f(z) = \int \frac{dz}{\left[z^\beta - \left(\frac{\mu_n \cdot I_D}{v_s} \right)^\beta \right]^{1/\beta}} \quad (6b)$$

Similar to the accumulation layer A, the voltage drop over the region C can easily be calculated:

$$V_C = \frac{I_D \cdot \left(W_T - W_A - \frac{L_p}{2} \cdot tg\alpha \right)}{\left\{ [e \cdot W \cdot N_D \cdot \mu_n (L_d + L_p)]^\beta - \left(\frac{\mu_n \cdot I_D}{v_s} \right)^\beta \right\}^{1/\beta}}$$

drop over the whole drift region turns out to be:

$$V_{drift} = V_A + V_B + V_C \quad (8)$$

and is calculated by means of relations (4c), (5d) and (7). In each of these expressions, low field electron mobility μ_n , saturation velocity v_s and the curvature coefficient β in overall formula (3), play an important role. As already mentioned these coefficients show considerable level of anisotropy, i. e. their values for \underline{c} - direction and for \underline{a} and \underline{b} directions are remarkably different. Same parameters also depend on temperature. Low field mobility has been taken from state - of - the art measurements and lined by the following expressions [4], [5]:

$$\mu_{n\perp c} = 40 + \frac{350 \cdot \left(\frac{T}{300} \right)^{-2.4} - 40}{1 + \left(\frac{T}{300} \right)^{-0.76} \cdot \left(\frac{N_D}{2 \cdot 10^{17}} \right)^{0.76}} \frac{cm^2}{Vs} \quad (9a)$$

$$\mu_{n\parallel c} = 48 + \frac{1140 \cdot \left(\frac{T}{300} \right)^{-2.4} - 48}{1 + \left(\frac{T}{300} \right)^{-0.76} \cdot \left(\frac{N_D}{2 \cdot 10^{17}} \right)^{0.76}} \frac{cm^2}{Vs} \quad (9b)$$

The high field mobility parameters ν_s , β are extracted from the full band Monte-Carlo simulations and can be comprised by following formulae:

$$\nu_{s\perp c} = \frac{2.77 \cdot 10^7}{1 + 0.23 \cdot e^{\left(\frac{T}{600}\right)}} \frac{cm}{s} \quad (10a)$$

$$\nu_{\parallel c} = \frac{2.55 \cdot 10^7}{1 + 0.30 \cdot e^{\left(\frac{T}{600}\right)}} \frac{cm}{s} \quad (10a)$$

$$\beta_{\perp c} = 0.60 + 1 \cdot 10^{-3} \cdot T \quad (11a)$$

$$\beta_{\parallel c} = 0.01 + 1 \cdot 10^{-3} \cdot T \quad (11b)$$

The expressions (9), (10) and (11) have been inserted into main relations of the developed model ((4c), (5d) and (7)) and so far the drift region voltage drops in various cases have been calculated.

3. Numerical Results and Discussion

The model described above is accompanied with structure parameters used in this simulation (and usually met in the relevant references [2]):

$$W = 400\mu m \quad L_d = 20\mu m$$

$$W_A = 32\mu m \quad L_p = 50\mu m$$

$$W_T = 70\mu m$$

$$N_D = 4 \times 10^{21} m^{-3}$$

The model itself regards some general remarks:

- a) for a specific value of drift current I_D , the drift region voltage drop V_{DRIFT} is still proportional to μ_n^{-1} ;
- b) drift region voltage drop V_{DRIFT} should decrease if saturation velocity v_s increased;
- c) current parameter β models the shape of the $I_D(V_{DRIFT})$ (V_{DRIFT}) characteristic and thus makes a considerable influence on specific values.

The results of the calculation performed according to the proposed model are given in figures 2 and 3. The figure 2 exposes the effect of anisotropy for different values of temperature with the main consequences:

- for each value of temperature, the "normal" orientation ($\perp c$) provides larger values of quasi-saturation drain current I_{Dqs} compared to parallel orientation ($\parallel c$);
- for each value of temperature, the characteristic $I_D(V_{DRIFT})$ has a bigger slope for small values of drain current in the case of "parallel" orientation ($\parallel c$) than in the case of "normal" orientation ($\perp c$);
- for higher values of drain current, the situation turns out to be quite different (due to the anisotropy of the curvature coefficient β); the slope of the characteristic suddenly becomes smaller in the case of "parallel" orientation ($\parallel c$) compared to the case of "normal" orientation ($\perp c$), thus resulting in the smaller values of quasi-saturation current for "parallel" orientation ($\parallel c$) compared to the latter one ($\perp c$).

The figure 3 shows $I_D(V_{drift})$ characteristic calculated for different values of temperature for each of the investigated orientations. In both cases, for the same value of drain current, the drift region voltage drop remarkably increases with the increase of temperature, mostly due to the μ_n^{-1} dependence described above.

So far only the characteristic drain current versus drift region voltage drop has been considered. Naturally, drain current has its upper cut-off caused by the channel saturation appearance. For gate voltage values usually met in such structures the section of the characteristic concerning small values of drain current (and drift region voltage drop consequently) is expected to play an important role. The drain current values comparable to quasi-saturation one (inevitably accompanied for greater gate voltages) appears rather as an exception.

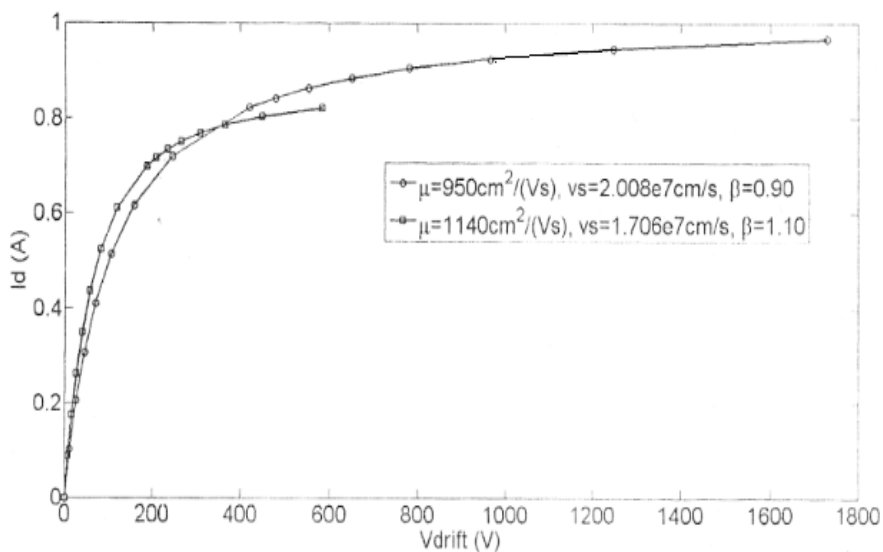


Figure 2a: Drain current versus drift region voltage drop- the influence on anisotropy (temperature=300K)

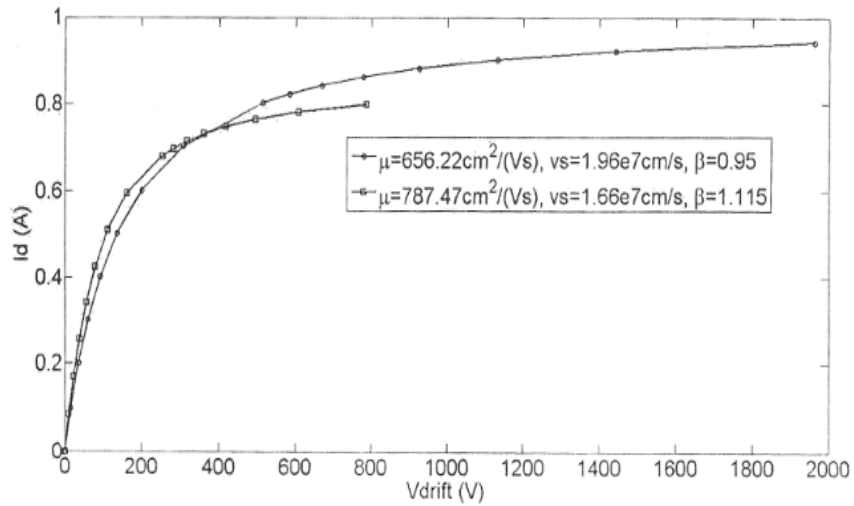


Figure 2b: Drain current versus drift region voltage drop- the influence on anisotropy (temperature=350K)

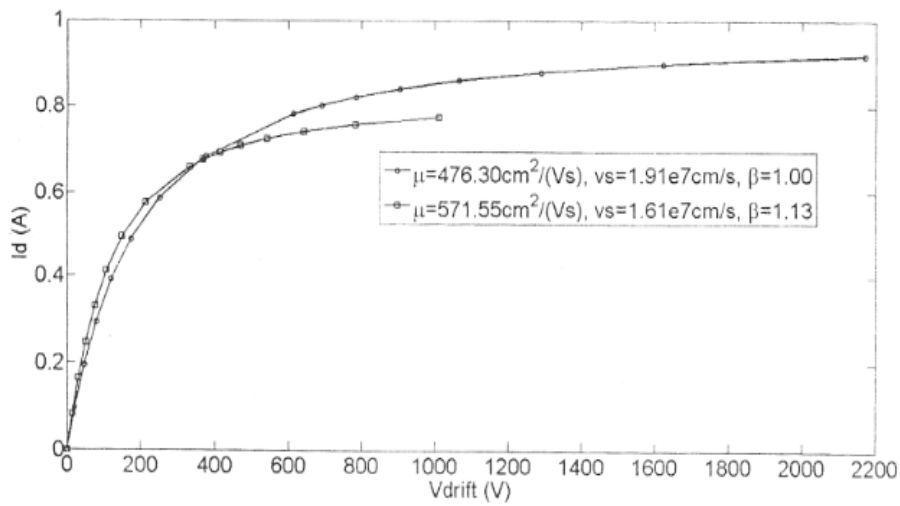


Figure 2c: Drain current versus drift region voltage drop- the influence on anisotropy (temperature=400K)

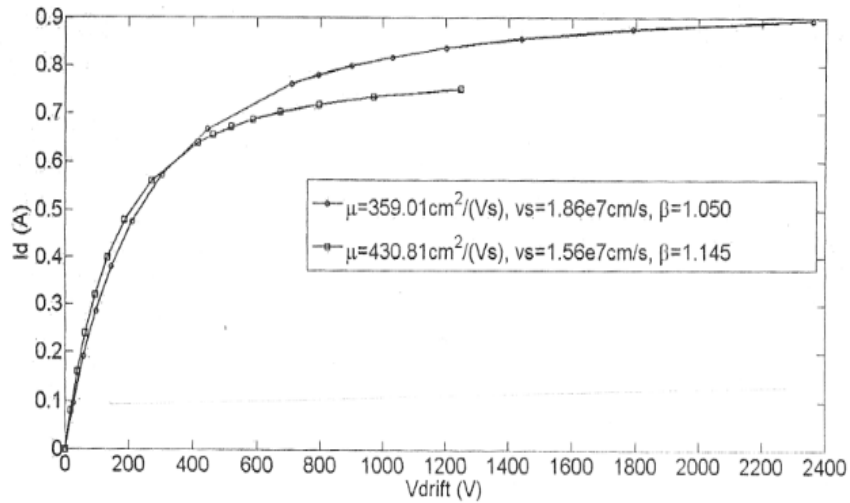


Figure 2d: Drain current versus drift region voltage drop- the influence on anisotropy (temperature=450K)

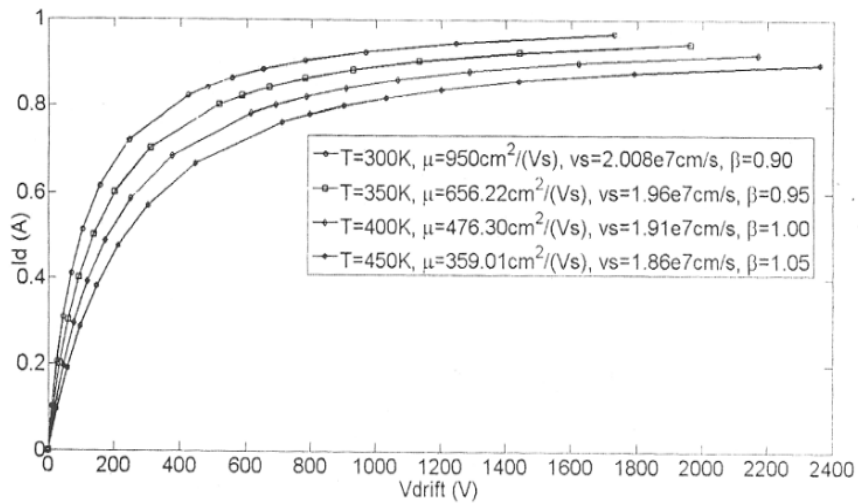


Figure 3a .Drain current versus drift region voltage drop for different values of temperature ("normal" orientation \perp c))

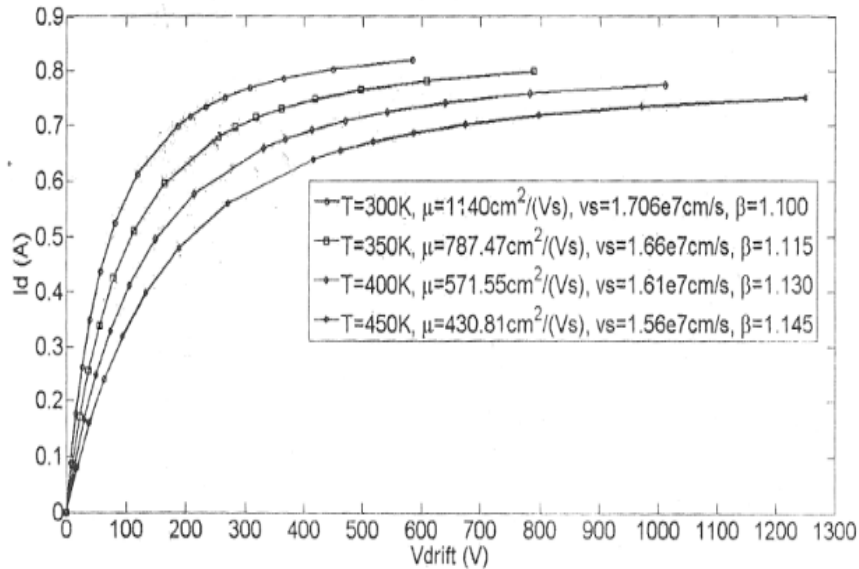


Figure 3b. Drain current versus drift region voltage drop for different values of temperature ("parallel" orientation (c))

4. Conclusions

This paper has given its contribution to the improvement of the existing theory of VDIMOS by introducing more accurate transport model including the fine tuning curvature coefficient. By means of such developed model, the drift region voltage drop has successfully been calculated. The coefficient, as well as saturation velocity and low electric field mobility possess a considerable level of anisotropy, which mainly affected the steepness of calculated current-voltage characteristics. It has also been proven that the change of working temperature strongly affected the investigated characteristics. This way obtained expressions form an adequate basis for constructing final model of VDIMOS, i.e. unification with the model describing channel.

References

- [1] MD Hasanuzzaman, Sred K. Islam, Leon M. Tolbert, Burak Ozpineci: "Design, Modelling , Testing and Spice Parameter Extracting of Transistor in 4H-Silicon Carbide", *Frontiers in Electronics*, pp. 733.-746.,2005.
- [2] A. Elasser and T.P. Chow, "Silicon Carbide Benefits and Advantages for Power Electronics Circuits and Systems," *Proc. IEEE*, 2002: 90(6): 969-86.
- [3] Zau J., D kotchetkov and AA Balankin "Thermal conductivity of GaN films: Effects of impurities and dislocations" *Journal of Applied Physics* 92, (2002) p.2534
- [4] A. Power and L. Rowland: "SiC Materials- Progress, Status and Potential Roadblocks, *Processing IEEE*, pp.942.-955.,90(6).2002.
- [5] J.R. Brews, A charge sheet model of the MOSFET, *Solid State Electron.* 21 (1978) 345–355.
- [6] M . Roschke, F. Schwierz, Electron mobility model for 4H, 6H and 3C SiC, *IEEE Trans. Electron Dev.* 48 (2001) 1442–1447.
- [7] Hasanuzzaman M, Islam SK, Tolbert LM, Ozpineci B. Model simulation and verification of a vertical double implanted (DIMOS) transistor in 4H-SiC, In: *Proc the IASTED International Conference on Power System Palm Spring 2003* p. 313–6.
- [8] Nakashima and H.Harima, "Characterization of structural and electrical properties in SiC by Raman spectroscopy", in *Inst. Phys. Conf. Series*, p. 269,(1969).
- [9] T. Kinoshita, K. Muto, M. Schadt, G. Pensl, and K. Takeda,"Calculation of the anisotropy of the Hall mobility in N-type 4H- and 6H-SiC", *Mat. Sci. Forum*, vols.264-268,p.295,1998.
- [10] M. Schadt, G. Pensl. R . P. Devaty, W, J , Choyke, R. Stein. And D. Stephany, "Anisortropy of the electron Hall in 4H,6H,

- Choyke, and 15R silicon carbide", *Appl. Phys. Lett.*, vol. 65, p. 3120.1994.
- [11] Krishna Shenai, Effect of P-Base sheet and contact Resistances on Static current-voltage Characteristics of Scaled low-voltage Vertical Power DMOSFETs, *IEEE Electron Devices Letters*, no. 6, pp. 270-272,1991.
- [12] Hasanuzzaman M, Islam S K, Tolbert L M and Ozpineci B 2002 Analytical modelling of vertical double implanted power MOSFET (DIMOS) in 4H-SiC *Proc. of Connecticut Symp. on Microelectronics and Optoelectronics Connecticut Marc.*
- [13] Hasanuzzaman M D, Islam S K, Tolbert L M and Ozpineci B 2005 Design, modeling, testing and spice parameter extraction of DIMOS transistor in 4H-SiC *Front. Electron.* 733–46.